

Phase diagram and complexity of mode-locked lasers: from order to disorder

L. Leuzzi^{1,3}, C. Conti^{2,3}, V. Folli³, L. Angelani^{1,3}, G. Ruocco^{2,3}

¹Research center SMC INFM-CNR, c/o Università di Roma “Sapienza,” I-00185, Roma, Italy

²Research center Soft INFM-CNR, c/o Università di Roma “Sapienza,” I-00185, Roma, Italy

³Dipartimento di Fisica, Università di Roma “Sapienza,” I-00185, Roma, Italy

We investigate mode-locking processes in lasers displaying a variable degree of structural randomness, from standard optical cavities to multiple-scattering media. By employing methods mutated from spin-glass theory, we analyze the mean-field Hamiltonian and derive a phase-diagram in terms of the pumping rate and the degree of disorder. Three phases are found: i) paramagnetic, corresponding to a noisy continuous wave emission, ii) ferromagnetic, that describes the standard passive mode-locking, and iii) the spin-glass in which the phases of the electromagnetic field are frozen in an exponentially large number of configurations. The way the mode-locking threshold is affected by the amount of disorder is quantified. The results are also relevant for other physical systems displaying a random Hamiltonian, like Bose-Einstein condensates and nonlinear optical beams.

The number of different disciplines converging in the field of disordered lasers is impressive; random lasers embrace photonics [1], wave-transport and localization [2, 3, 4, 5], spin-glass theory [6], random-matrices [7], soft- and bio-matter [8, 9, 10], nonlinear and quantum physics [11, 12, 13, 14, 15, 16]. Notwithstanding the several theoretical and experimental investigations, as recently reviewed in [1, 17], many are the open issues and, certainly, the development of the field cannot be compared with that of standard lasers (SL) (i.e., those not displaying structural disorder), even if the first theoretical prediction of RL [18] is dated not very far from the first theoretical work on SL [19]. In this respect, a comprehensive theory of stimulated emission able to range from ordered to disordered lasers will be certainly an important step. This theory should be able to account for the strength of disorder as a parameter and should predict specific regimes attainable in SL and RL. At the moment such a theory is not available, and the literature dealing with the two kinds of lasers is still largely disjoint. Furthermore, nano-structured lasers unavoidably display some degree of disorder due to fabrication tolerances; hence understanding the effect of randomness in the light emission has important practical relevance. The main question addressed in this work is the following: consider a SL operating in mode-locking (ML) and progressively increase the amount of structural disorder, at which value one should expect that the mode-locking is frustrated? Which kind of states are expected?

In this manuscript we derive a self-consistent theoretical approach to ML in ordered and disordered lasers; we make use of all the machinery inherited from spin-glass theory [20], at the moment the only mathematical technique enabling to fully account for different degree of randomness and for several other phenomena expected in complex systems. We report on a phase-diagram for ML in lasers unveiling the interplay between randomness and nonlinearity. We discover the existence of different phases characterized by a non-trivial configurational entropy, or *complexity*, which measures the number of energetically equivalent ML states.

Previous theoretical work, which was based on ther-

modynamic approaches, has dealt with the two regimes: the ordered case where the ML is demonstrated to be given by a ferromagnetic-like transition [21, 22, 23] and the completely disordered limit [6]. The former case being relevant to fiber or dye/solid-state standard passive ML [24]; the latter being more oriented on stimulated emission in the presence of multiple scattering [17, 25]. Our analysis unifies the scenario, by showing that it is possible to treat in a single systematic way ML processes in the presence of an arbitrary degree of disorder. The study is based on the following steps: 1) perform a statistical average of the disordered free-energy of the system; 2) identify the order parameters; 3) determine the thermodynamic free-energy; 4) build the phase-diagram; 5) compute the complexity.

Our main finding can be summarized as follows: the self-starting ML process maintains its standard “ferromagnetic” character (i.e., an abrupt transition from a continuous wave operation to a pulsed regime) as far as the structural fluctuations are sensitively smaller than the average value of the mode coupling coefficients, although the pumping threshold for passive ML grows with the amount of disorder. Conversely, for large disorder the transition acquires a glassy character, the pumping threshold becomes independent of the “disorder to order” ratio and the complexity is not vanishing; this implies that there exists a large number of ML states distributed in a given free energy interval and large fluctuations from pulse to pulse are expected. Also an intermediate regime occurs, where the system maintains a ferromagnetic behavior but a non-zero complexity is found.

Leading model — Under general hypotheses (discussed with details in [26, 27]) the mode-phase dynamics of a RL can be cast into a dynamical problem with a random Hamiltonian

$$\mathcal{H}_J[\phi] = - \sum_{\substack{i_1 < i_2, j_1 < j_2 \\ i_1 < j_1}}^N J_{\mathbf{i}\mathbf{j}} \cos(\phi_{i_1} + \phi_{i_2} - \phi_{j_1} - \phi_{j_2}) \quad (1)$$

where N is the number of electromagnetic modes, ϕ_i are their phases, $\mathbf{i} = (i_1, i_2)$ and the quenched cou-

plings have a Gaussian distribution with $\overline{J_{ij}} = J_0/N^3$ and $\overline{(J_{ij} - \overline{J_{ij}})^2} = \sigma_J^2/N^3$. The overbar denotes the average over the disorder, which is quantified by the parameter $R_J \equiv \sigma_J/J_0$ that is the ratio between the standard deviation of the distribution of the coupling coefficients J_{ij} and their mean. The limit $R_J \rightarrow 0$ ($R_J \rightarrow \infty$) corresponds to the ordered (disordered) case. The other relevant parameter is the normalized pumping threshold for mode-locking [26] \mathcal{P} , that is connected to the thermodynamic inverse temperature β and to the interactions by the relationship $\mathcal{P} = \sqrt{\beta J_0} = \sqrt{\beta/R_J}$, where $\bar{\beta} = \beta \sigma_J$. In our units, when $R_J \rightarrow 0$, $p = p_{ord} \cong 3.339$ (see Fig.1), in agreement with the ordered case [6][32]; as detailed below, the deviation from this value quantifies an increase of the standard mode-locking threshold p_{ord} due to disorder. The specific value for p_{ord} will depend on the class of lasers under consideration (e.g., a fiber loop laser or a random laser with paint pigments), but the trend of the passive mode-locking threshold with the strength of disorder R_J in Fig.1 (FM/PM transition line, see below) has a universal character.

Averaged free-energy — The average free energy is calculated by the replica trick [20]. By considering n copies of the system, Eq. (1), the free energy averaged over the disorder can be computed as

$$\beta\Phi = -\frac{1}{N} \overline{\log Z_J} = -\frac{1}{N} \lim_{n \rightarrow 0} \frac{\overline{Z_J^n} - 1}{n}. \quad (2)$$

The thus *replicated* partition function, $\overline{Z_J^n}$, takes the form

$$\overline{Z_J^n} \propto \int \mathcal{D}\mathbf{X} \exp[-nNG(\mathbf{X})] \sim e^{-nNG(\mathbf{X}_{SP})} \quad (3)$$

where \mathbf{X} denotes the set of all the order parameters and the integral is evaluated by means of the saddle point approximation (valid for large N).

Spin-glass systems described by more-than-two-body interactions, cf. Eq. (1), are known to have low temperature phases whose correct thermodynamic description is provided by the so-called one step Replica Symmetry Breaking (1RSB) Ansatz [28, 29]. Under this Ansatz, taking the $n \rightarrow 0$ limit, the free energy functional reads [33]

$$\begin{aligned} \beta\Phi = & -\frac{\bar{\beta}R_J}{8} |\tilde{m}|^4 - \frac{\bar{\beta}^2}{32} \left[1 - (1-m)(|q_1|^4 + |r_1|^4) \right] \quad (4) \\ & -m(|q_0|^4 + |r_0|^4) + |r_d|^2 - \Re \left[\frac{1-m}{2} (\bar{\lambda}_1 q_1 + \bar{\mu}_1 r_1) \right. \\ & \left. + \frac{m}{2} (\bar{\lambda}_0 q_0 + \bar{\mu}_0 r_0) - \bar{\mu}_d r_d - \bar{\nu} \tilde{m} \right] + \frac{\lambda_1^R}{2} \\ & - \frac{1}{m} \int \mathcal{D}[\mathbf{0}] \log \int \mathcal{D}[\mathbf{1}] \left[\int_0^{2\pi} d\phi \exp \mathcal{L}(\phi; \mathbf{0}, \mathbf{1}) \right]^m \end{aligned}$$

where $\mathbf{0} = \{x_0, \zeta_0^R, \zeta_0^I\}$, $\mathbf{1} = \{x_1, \zeta_1^R, \zeta_1^I\}$, $\mathcal{D}[\mathbf{a}]$ is the product of three Normal distributions and

$$\begin{aligned} \mathcal{L}(\phi; \mathbf{0}, \mathbf{1}) \equiv & \Re \left\{ e^{i\phi} \left[\bar{\zeta}_1 \sqrt{\Delta \lambda^R - |\Delta \mu|} + \bar{\zeta}_0 \sqrt{\lambda_0^R - |\mu_0|} + \right. \right. \\ & \left. \left. x_1 \sqrt{2\Delta \bar{\mu}} + x_0 \sqrt{2\bar{\mu}_0} + \bar{\nu} \right] + e^{2i\phi} \left(\bar{\mu}_d - \frac{\bar{\mu}_1}{2} \right) \right\} \quad (5) \end{aligned}$$

with $\Delta \lambda = \lambda_1 - \lambda_0$, $\Delta \mu = \mu_1 - \mu_0$. For later convenience we define the following averages over the action $e^{\mathcal{L}}$, cf. Eq. (5): $c_{\mathcal{L}} \equiv \langle \cos \phi \rangle_{\mathcal{L}}$, $s_{\mathcal{L}} \equiv \langle \sin \phi \rangle_{\mathcal{L}}$.

The values of the order parameters $\lambda_{0,1}, \mu_{0,1}, \mu_d$ and ν are yielded by

$$\lambda_{0,1} = \frac{\bar{\beta}^2}{4} (q_{0,1})^3; \quad \mu_{0,1} = \frac{\bar{\beta}^2}{4} |r_{0,1}|^2 r_{0,1} \quad (6)$$

$$\mu_d = \frac{\bar{\beta}^2}{8} |r_d|^2 r_d; \quad \nu = \frac{\bar{\beta} R_J}{2} |\tilde{m}|^2 \tilde{m} \quad (7)$$

The remaining parameters are obtained by solving the self-consistency equations:

$$q_1 = \langle \langle c_{\mathcal{L}}^2 \rangle_m \rangle_{\mathbf{0}} + \langle \langle s_{\mathcal{L}}^2 \rangle_m \rangle_{\mathbf{0}} \quad (8)$$

$$q_0 = \langle \langle c_{\mathcal{L}}^2 \rangle_m \rangle_{\mathbf{0}} + \langle \langle s_{\mathcal{L}}^2 \rangle_m \rangle_{\mathbf{0}} \quad (9)$$

$$r_1 = \langle \langle c_{\mathcal{L}}^2 \rangle_m \rangle_{\mathbf{0}} - \langle \langle s_{\mathcal{L}}^2 \rangle_m \rangle_{\mathbf{0}} + 2i \langle \langle c_{\mathcal{L}} s_{\mathcal{L}} \rangle_m \rangle_{\mathbf{0}} \quad (10)$$

$$r_0 = \langle \langle c_{\mathcal{L}}^2 \rangle_m \rangle_{\mathbf{0}} - \langle \langle s_{\mathcal{L}}^2 \rangle_m \rangle_{\mathbf{0}} + 2i \langle \langle c_{\mathcal{L}} \rangle_m \rangle_{\mathbf{0}} \langle \langle s_{\mathcal{L}} \rangle_m \rangle_{\mathbf{0}} \quad (11)$$

$$r_d = \langle \langle \langle e^{2i\phi} \rangle_{\mathcal{L}} \rangle_m \rangle_{\mathbf{0}}; \quad \tilde{m} = \langle \langle \langle e^{i\phi} \rangle_{\mathcal{L}} \rangle_m \rangle_{\mathbf{0}} \quad (12)$$

where

$$\langle \langle \dots \rangle_m \rangle \equiv \frac{\int \mathcal{D}[\mathbf{1}] (\dots) \left[\int_0^{2\pi} d\phi e^{\mathcal{L}(\phi; \mathbf{0}, \mathbf{1})} \right]^m}{\int \mathcal{D}[\mathbf{1}] \left[\int_0^{2\pi} d\phi e^{\mathcal{L}(\phi; \mathbf{0}, \mathbf{1})} \right]^m} \quad (13)$$

$$\langle \langle \dots \rangle_{\mathbf{0}} \rangle \equiv \int \mathcal{D}[\mathbf{0}] (\dots) \quad (14)$$

The overlap parameters $q_{0,1}$ are real-valued, whereas $r_{0,1}, r_d$ and \tilde{m} are complex. ‘‘One step’’ parameters $X_{0,1}$ ($X = q, r$) enter with a probability distribution that can be parametrized by the so-called replica symmetry breaking parameter m , such that, e.g., $P(X) = m \delta(X - X_0) + (1 - m) \delta(X - X_1)$.

Complexity — The resulting eleven independent parameters that can be evaluated by solving Eqs. (8)-(12) must be combined with a further equation for the parameter m . This is strictly linked to the expression for the *complexity* function of the system, i.e., the average logarithm of the number of states of the system present at a given free energy level f . The complexity can be computed, e.g., as the Legendre transform of the replicated free energy, Eq. (4):

$$\begin{aligned} \Sigma = & \min_m [-\beta m \Phi(m) + \beta m f] = \beta m^2 \frac{\partial \Phi}{\partial m} \quad (15) \\ = & \frac{3}{4} \beta^2 m^2 (|q_1|^4 + |r_1|^4 - |q_0|^4 - |r_0|^4) \\ & + \int \mathcal{D}[\mathbf{0}] \log \int \mathcal{D}[\mathbf{1}] \left[\int_0^{2\pi} d\phi \exp \mathcal{L}(\phi; \mathbf{0}, \mathbf{1}) \right]^m \\ & - m \int \mathcal{D}[\mathbf{0}] \langle \log \int_0^{2\pi} d\phi \exp \mathcal{L}(\phi; \mathbf{0}, \mathbf{1}) \rangle_m \end{aligned}$$

where the single state free energy $f = \partial(m\Phi)/\partial m$ is conjugated to m . Since the above expression is proportional to $\partial\Phi/\partial m$, equating $\Sigma = 0$ provides the missing equation to determine the order parameters values.

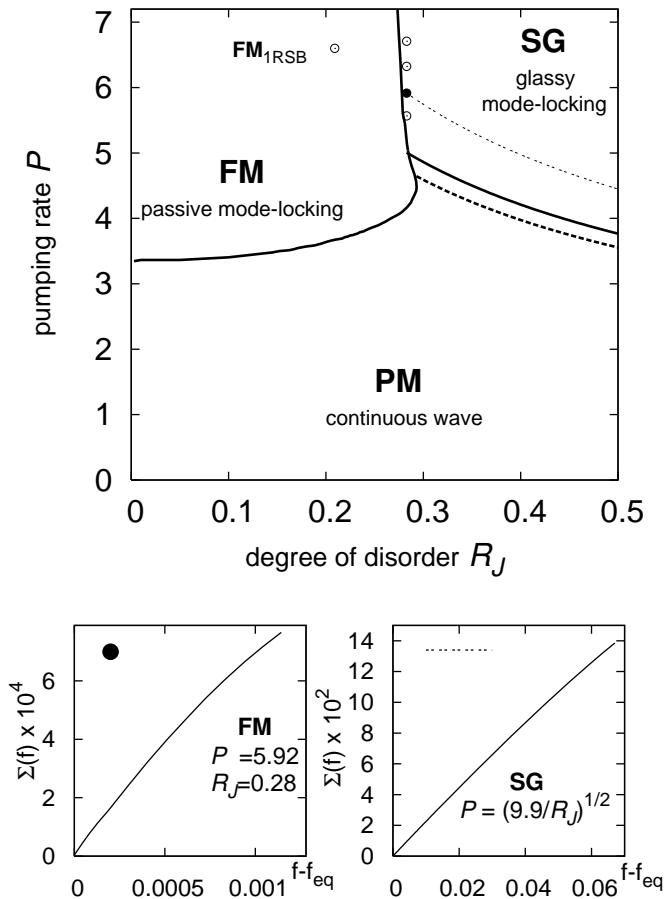


FIG. 1: Phase diagram in the plane (R_J, \mathcal{P}) . Three phases are found: PM (low \mathcal{P}), FM (high \mathcal{P} /weak disorder) and SG (high \mathcal{P} /strong disorder). The full line is thermodynamic transitions, the dashed line represents the dynamic PM/SG transition. The transition line to the FM phase (both from PM and from SG) are obtained using the RS approximation. The circles are exact 1RSB FM solutions. In the insets complexity vs. free energy curves are plotted in the SG phase (right inset, at $\bar{\beta} = 9.9$, R_J independent; in the main plot: $p = \sqrt{9.9/R_J}$, tiny-dashed line) and in the FM phase next to the SG/FM transition (left inset, at $R_J = 0.28$, $\mathcal{P} = 5.92$; full circle in the main plot). The latter is two order of magnitude smaller.

Phase-diagram — By varying the normalized pumping rate \mathcal{P} and degree of disorder R_J , we find three different phases, as shown in Fig. 1. For low \mathcal{P} and R_J the only phase present is completely disordered: all order parameters are zero and we have a “paramagnet” (PM); the laser emission is expected to be given by a noisy continuous wave emission, and all the mode-phases are uncorrelated. The PM exists everywhere in the whole plane (R_J, \mathcal{P}) , becoming thermodynamically subdominant as \mathcal{P} and R_J increase and other phases arise. For large disorder, as the pumping rate is increased, a discontinuous transition occurs from the PM to a spin-glass (SG) phase in which

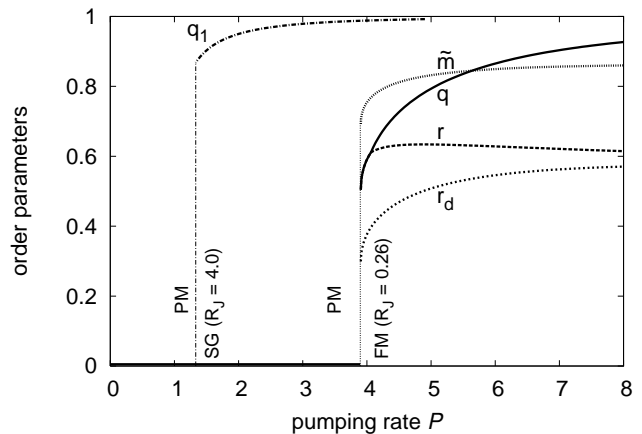


FIG. 2: Discontinuity of the order parameters at the transition point in the pumping rate p . Left: jump in q_1 at the PM/SG ($R_J = 4.0$). Right: Discontinuous \tilde{m} , r , q , r_d at the PM/FM transition ($R_J = 0.26$). In the FM phase the thermodynamics is computed in the RS approximation ($q_1 = q_0 = q$, $r_1 = r_0 = r$).

the phases ϕ are frozen at given values, though not displaying any ordered pattern in space. First, along the line $\mathcal{P}_d = \sqrt{\beta_d/R_J}$ ($\beta_d = 6.322$), a dynamic transition occurs (dashed line). Indeed, the lifetime of metastable states is infinite in the mean-field model and the dynamics gets stuck in the highest lying excited states. The thermodynamic (lowest energy) state is, however, still PM. Across the full line (cf. Fig. 1) $\mathcal{P}_s = \sqrt{\beta_s/R_J}$ ($\beta_s = 7.094$) a true thermodynamic phase transition to the SG phase occurs. The order parameter q_1 , else called Edwards-Anderson parameter q_{EA} [30] discontinuously jumps at the transition to a non-zero value $q_1 > q_0 = 0$ and $\tilde{m} = r_0 = r_1 = r_d = 0$ (see Fig. 2). The SG phase exists for any value of R_J and $\bar{\beta} > \bar{\beta}_s$. However, for small R_J , a ferromagnetic (FM) phase turns out to dominate over the SG and the PM phases. The transition line PM/FM is the standard passive ML threshold (see e.g. [27, 31]) and from Fig.1 we see that it takes place at growing pumping rates for increasing disorder, as far as the SG is not encountered.

To precisely describe the FM phase in the 1RSB Ansatz we have to solve eleven coupled integral equations [Eqs. (8)-(12) and $\Sigma = 0$, cf. Eq. (15)]. In the region where this $\text{FM}_{1\text{rsb}}$ phase is the thermodynamically dominant solution, however, the PM and the SG solutions also satisfy the same set of equations. Starting the iterative resolution with randomly chosen initial conditions, determining the SG/ $\text{FM}_{1\text{rsb}}$ and the PM/ $\text{FM}_{1\text{rsb}}$ transition lines becomes numerically very demanding. An approximation is obtained by considering the Replica Symmetric (RS) solution for the FM phase (FM_{rs}). This reduces the number of independent parameters to five ($q_1 = q_0$, $r_1^{R,I} = r_0^{R,I}$, r_d and \tilde{m}). The corresponding transition line is shown in Fig. 1. The exact FM phase is provided by a 1RSB

solution and some sampled points are represented by the circles in the phase diagram.

The 1RSB ansatz also enables to determine the not-vanishing extensive complexity, which signals the presence of a huge quantity of excited states with respect to ground states. This also implies the occurrence of dynamic transitions besides the thermodynamic one, as anticipated. These take place between PM and SG [where the state structure always displays a non-trivial $\Sigma(f)$ for any $\bar{\beta} > \bar{\beta}_d$] and in the FM phase, though the magnitude of Σ turns out to be smaller. In the left inset of Fig. 1 we show, e.g., $\Sigma(f)$ in the FM_{1RSB} phase at $(R_J, \mathcal{P}) = (0.28, 5.92)$. This has to be compared with the SG complexity at the same temperature (right inset of Fig. 1) that is sensitively larger and does not depend on the “disorder/order ratio”: the maximum complexity drops of about two order of magnitude at the SG/FM_{1RSB} transition, thus unveiling a corresponding *high to low complexity transition*.

Conclusion — We have reported on what we believe to be the first comprehensive theoretical treatment of ML processes in lasers with structural disorder. Our approach enables to take into account an arbitrary strength of randomness in the system and results into a phase-diagram for random lasers. In this diagram, a

ferromagnetic-like (standard passive mode-locking) and glassy-like phases (“glassy” mode-locking) are present and determined by the pumping rate and by the degree of structural disorder. The way the self-starting passive mode-locking threshold is affected by the latter quantity has been quantified. This result can be experimentally tested in a variety of different physical systems, from laser powders to standard laser cavities, and is relevant for any nonlinear interaction process of several oscillators in the presence of disorder, also including Bose-Einstein condensation. The phase-diagram reveals a rich variety of different phases, and even if only those thermodynamically favored are reported above, the dynamics of the mode-locking process (and the corresponding synchronization of the nonlinearly coupled resonances) is expected to be strongly affected by the existence of several valleys in the free energy (described by a not vanishing *complexity*). In this respect, lasing in disordered system is an important framework for investigating out of equilibrium dynamical systems, including quantum effects.

Acknowledgments — The research leading to these results has received funding from the European Research Council under the European Community’s Seventh Framework Program (FP7/2007-2013)/ERC grant agreement n. 201766.

-
- [1] H. Cao, *Waves in Random Media and Complex Media* **13**, R1 (2003).
- [2] S. John and G. Pang, *Phys. Rev. A* **54**, 3642 (1996).
- [3] A. Lubatsch, J. Kroha, and K. Busch, *Phys. Rev. A* **71**, 184201 (2005).
- [4] D. S. Wiersma, M. P. Vanalbada, and A. Lagendijk, *Nature* **373**, 203 (1995).
- [5] S. Lepri, S. Cavalieri, G.-L. Oppo, and D. S. Wiersma, *Phys. Rev. A* **75**, 063820 (2007).
- [6] L. Angelani, C. Conti, G. Ruocco, and F. Zamponi, *Phys. Rev. Lett.* **96**, 065702 (2006).
- [7] C. W. J. Beenakker, *Phys. Rev. Lett.* **81**, 1829 (1998).
- [8] D. Zhang, B. Cheng, J. Yang, Y. Zhang, W. Hu, and Z. Li, *Optics Comm.* **118**, 462 (1995).
- [9] R. C. Polson and Z. V. Vardeny, *Appl. Phys. Lett.* **85**, 1289 (2004).
- [10] M. Siddique, R. R. Alfano, G. A. Berger, M. Kempe, and A. Z. Genack, *Opt. Lett.* **21**, 450 (1996).
- [11] L. Florescu and S. John, *Phys. Rev. Lett.* **93**, 013602 (2004).
- [12] L. I. Deych, *Phys. Rev. Lett.* **95**, 043902 (2005).
- [13] H. E. Tureci, L. Ge, S. Rotter, and A. D. Stone, *Science* **320**, 643 (2008).
- [14] M. Patra, *Phys. Rev. A* **65**, 043809 (2002).
- [15] G. Hackenbroich, C. Viviescas, B. Elattari, and F. Haake, *Phys. Rev. Lett.* **86**, 5262 (2001).
- [16] G. A. Berger, M. Kempe, and A. Z. Genack, *Phys. Rev. E* **56**, 6118 (1997).
- [17] D. S. Wiersma, *Nature Physics* **4**, 359 (2008).
- [18] R. Ambartsumyan, N. Basov, P. Kryukov, and S. Lethokov, *IEEE J. Quantum Electron.* **2**, 442 (1966).
- [19] A. L. Schawlow and C. H. Townes, *Phys. Rev.* **112**, 1940 (1958).
- [20] M. Mezard, G. Parisi, and M. A. Virasoro, *Spin Glass Theory and Beyond* (World Scientific, Singapore, 1987).
- [21] H. Haken, *Synergetics* (Springer-Verlag, Berlin, 1978).
- [22] R. Weill, A. Rosen, A. Gordon, O. Gat, and B. Fischer, *Phys. Rev. Lett.* **95**, 013903 (2005).
- [23] L. Angelani, C. Conti, L. Prignano, G. Ruocco, and F. Zamponi, *Phys. Rev. B* **76**, 064202 (2007).
- [24] H. A. Haus, *IEEE J. Select. Topics Quantum Electron.* **6**, 1173 (2000).
- [25] H. Cao, X. Jiang, Y. Ling, J. X. Xu, and C. M. Soukoulis, *Phys. Rev. B* **67**, 161101R (2003).
- [26] L. Angelani, C. Conti, G. Ruocco, and F. Zamponi, *Phys. Rev. B* **74**, 104207 (2006).
- [27] A. Gordon and B. Fischer, *Opt. Comm.* **223**, 151 (2003).
- [28] E. Gardner, *Nucl. Phys. B* **257**, 747 (1985).
- [29] A. Crisanti and H.-J. Sommers, *Z. Phys. B* **87**, 341 (1992).
- [30] S. Edwards and P. Anderson, *J. Phys. F* **5**, 965 (1975).
- [31] A. Gordon and B. Fischer, *Phys. Rev. Lett.* **89**, 103901 (2002).
- [32] A factor of 8 has to be considered because of the overcounting of terms in the Hamiltonian of the model studied in Ref. [6] with respect to Eq. (1). This factor can be absorbed into the temperature yielding the pumping threshold $p_{\text{ord}} = \sqrt{8/T_0} \cong 3.34$, where $T_0 \cong 0.717$ is the temperature at which the FM phase first appears in complete absence of disorder.
- [33] In Ref. [6] the standard deviation of the quenched disorder was fixed at $\sigma_J^2 = 8$. In this work the adimensional temperature introduced there is computed in units of σ_J .